Coupling of inverse method and cuckoo search algorithm for multiobjective optimization design of an axial flow pump

Mohamed Abdessamed Ait Chikh[1], Idir Belaidi[1], Sofiane Khelladi[2], Abderrachid Hamrani[3] and Farid Bakir[2]

Abstract

This work describes the application of a multiobjective cuckoo search method for turbomachinery design optimization of an axial pump. Maximization of the total efficiency and minimization of the required net positive suction head of the pump are the two objective functions considered for the optimization problem. The optimization process is carried out on a range of imposed volumetric flow rates, with taking into account at each discretized radius between the hub and tip of the rotor: the profile camber, rotor wall thickness, angular deviation, and the solidity, regarded as geometrical constraints and nominal flow rate as mechanical constraint. Two strategies are proposed in order to solve the problem. In the first one, three forms of mono-objective model with two variables, total efficiency and net positive suction head, are considered. In the second one, a multiobjective model with nondominated sorting scheme is adopted. A comparative evaluation of results obtained from the proposed approach with those of a reference machine and genetic algorithm allowed us to validate the present work.

Keywords

Axial flow pump design, multiobjective optimization, cuckoo search, nondominated sorting cuckoo search

Introduction

Classical methods used for turbomachinery design are generally based on empirical correlations that make very difficult to achieve the global optimal design. In recent years, thanks to the development of computational methods, a lower dependency on experimental correlations is observed.

As with most complex design problems, there are multiple performance metrics that one might seek to enhance and optimize in turbomachinery design. Considering the multi-objectivity of the optimization problem is more than necessary, and above all, unavoidable.

Usually, Pareto front[1] and aggregation approach[2] are the two main techniques employed for solving multiobjective optimization problem. In the Pareto front, a set of all optimal solutions, extracted from conflicting objectives, are represented in a surface or a curve known as a "front." Thus, this front helps us to understand the nature of trade-offs that needs to be made in order to select a good decision/solution. The second technique consists of aggregating the "multiobjective" problem into a single function. Each objective function represents the desired performance to be maximized or minimized.

Numerous works have been carried out in the general framework of design optimization of high performance turbomachines. One of the first research works in this field addressed the design of an axial flow compressor stage with the objective of minimizing the aerodynamic losses and the weight of the stage, while maximizing the compressor stall margin. The pitchline analysis and the throughflow calculation techniques with the Davidon–Fletcher–Powell minimization method are employed in the formulation of

[1]Laboratoire d'Energétique, Mécanique et Ingénierie, Université de Boumerdes, Boumerdes, Algeria
[2]Laboratoire de Dynamique des Fluides, Arts et Métiers ParisTech, Paris, France
[3]Department of Bioresource Engineering, McGill University, Montreal, Canada

Corresponding author:
Mohamed Abdessamed Ait Chikh, Laboratoire d'Energétique, Mécanique et Ingénierie, Université de Boumerdes, Boumerdes, Algeria.
Email: mohamed.aitchikh@gmail.com

the multivariable single objective function.[3,4] Another work[5] combines a geometry parameterization scheme with a CFD simulation and a multiobjective tabu search optimization algorithm, in order to improve the performance of turbomachinery blades design. In Benini[6] an approach was developed for transonic compressor multiobjective design optimization and applied to the three-dimensional NASA rotor 37 shape. Maximizing the isentropic efficiency of the rotor and its pressure ratio, using a constraint on the mass flow rate, was the two objectives of the multiobjective evolutionary optimization problem. Thereafter, several works have been published and these include CFD known to be expensive methods of design. Also, the coupling of the nondominated sorting genetic algorithm (NSGAII) or multiobjective genetic algorithms (MOGAs) with CFD for the multiobjective optimization of the 3D inverse design, is discussed in reference to the work of Samad and Kim[7] and Bonaiuti and Zangeneh.[8] The same optimization techniques, coupled with design of experiments (DoEs)[9,10] and back propagation neural network[11,12] schemes were used.

We may also mention some recent works: In Chenxing and Qian,[13] a model based on orthogonal DoEs and neural network, for predicting the centrifugal fan performance parameters, is used, and a MOGA for optimization of total pressure and efficiency of the fan, and the best combination of impeller structural parameters. In Meng et al.,[14] the approach of weighted grey relational analysis combined with response surface methodology (RSM) is used to optimize the centrifugal fan impeller parameters. Simulation models are based on Box–Behnken design method. In Stadler et al.,[15] an inverse aeroacoustic design methodology of axial fans driven by a genetic algorithm is proposed. The multiobjective problem includes: the sound pressure frequency spectrum for the minimization of noise, aerodynamic efficiency, and pressure head; simulation model is based on a meshless lattice-Boltzmann solver. In Yang and Xiao,[16] a multiobjective optimization strategy has been used for pump–turbine impellers design. A RSM model with a multiobjective evolutionary GA is applied to find a Pareto front for the final trade-off selection. In Huang et al.,[17] the NSGAII was improved by crowding distance dynamic technique and coupled with a neural network and 3D inverse design method in order to optimize the efficiency and head of mixed flow pump with keeping the meridional section fixed during the optimizations process.

In the light of the numerous and varied consulted works, the difficulty of ensuring the overall optimum remains a problem posed and topical. Moreover, despite the existence of numerous and efficient metaheuristic methods, of bio- or socio-inspired type, the application of genetic algorithms in the different approaches remains preponderant. Bio- and socio-inspired methods remain poorly known in engineering applications.

This work contains three main contributions: first, a new approach of axial flow pump optimization design based on inverse design and nondominated sorting cuckoo search (CS); second, a new form of multiobjective optimization using single function; finally, a comparative study between nondominated sorting cuckoo search (NSCS) and NSGAII in turbomachinery design.

In this paper we propose a multiobjective optimization approach of a mono-rotor pump defined by a set of decision variables of geometrical and mechanical types, in order to minimize the net positive suction head (NPSHC) and maximize the total nominal efficiency over a range of the volumetric flow rate, compared with a reference pump. Thus, we have implemented two approaches: the first one is based on a single objective function, using the standard CS algorithm, with the penalty method.[18] The second approach deals with the problem of multiobjective optimization based on Pareto front and ''nondominated sorting cuckoo search,'' coupled with an inverse design approach, taking into account a very high number of geometric constraints that are solved by the feasible and nonfeasible method.[19]

The two proposed approaches were assessed by studying two cases, the first one takes into consideration eight decision variables, namely: initial volumetric flow rate, internal and external radius at the entrance and the exit of the rotor, the diffusion factor at the hub and the tip of the blade, and the number of blades. The value of the rotational speed considered in this first case is that of the reference machine. In the second case, six variables were considered, including the rotational speed, the external radius at the entrance and the exit of the rotor, the diffusion factor at the hub and the tip of the rotor, the number of blades. In the latter case, the initial volume flow rate and internal radius are that of the reference machine. The results of NSCS were compared to those of NSGAII. Finally, in both cases we used forced vortex.

Design model of an axial pump

As presented in Ait Chikh et al.,[20] two methods are commonly used for designing turbomachines: the inverse method for the design of new machine, and the direct method for analyzing the performance of an existing machine.

Inverse design approach

By applying the Euler theorem, and from the data, such as rotational speed, head (manometric height), volumetric flow rate, hub and tip radius at the entrance and exit of turbomachine, and the diffusion factors at tip and hub of the blade, and the number of blades of the rotor, the velocity triangles (Figure 1) for a selected type of vortex are calculated for each

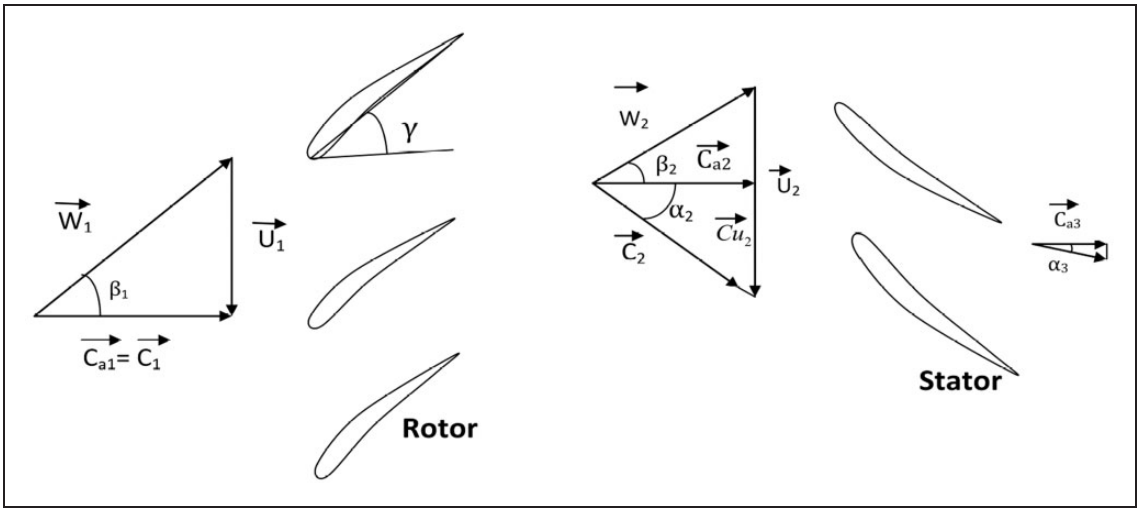

Figure 1. Velocity triangles of the axial flow pump.

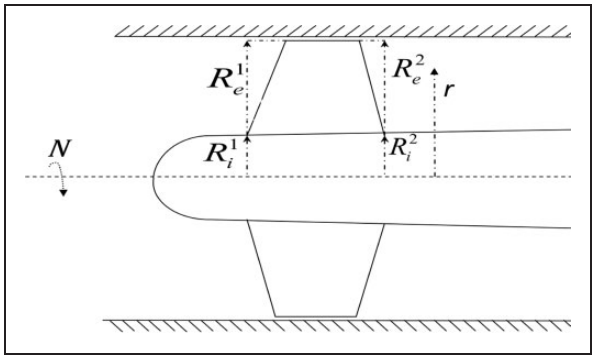

Figure 2. Geometrical parameters of an axial flow turbomachine.

section of the radial discretization between the shroud and the hub of the rotor (Figure 2). The tangential velocity $C_{u2}(r)$ is chosen by the user, depending on the available vortex model, for the forced vortex $C_{u2}(r) = rK$ and $K = gH/(\omega\eta_H((R_i^2 + R_e^2)/2)^2)$, with ω, g, and η_H are the angular velocity, gravity acceleration, and hydraulic efficiency, respectively. The geometrical characteristics of the rotor can be obtained by solving the inverse problem 1D, with an estimated η_H of 70%. The shape most suited to the velocity triangles is defined. To define the overall geometry of the pump blades, at each radius between the hub and the tip, some geometrical parameters should be defined: the chord, camber, stagger angle, and the maximum thickness of the profile. Using the normalized data of a NACA65, the geometry of the blade can be defined. The camber, incidence, and solidity are determined by using empirical correlation of the cited type profile.

Performance analysis

Performance analysis is a key step in the optimization process. It is based on the notion of the individual's fitness obtained from an analysis of the performances of an existing machine at a given range of volumetric flow rates in order to determine the nominal point, and then the characteristics of the machine in off-design. The real fluid effects are taken into account, such as pressure drops in the boundary layers near the wall (hub, shroud) and loss laws (incidence, friction, flow leakage, etc.) were used, see Robert et al.[21,22] for more details concerning the chosen approach. In addition, the slack distance (distance between the hub of the rotor and the shroud) is estimated equal to 5.0e-4 m.

Proposed design optimization approach

Formulation of the multiobjective optimization problem

We briefly recall the general mathematical formulation of the problem of mono-objective optimization and multiobjective optimization:

1. **Single objective cases**:

$$\begin{aligned} &\min \quad f(X) \\ &\textit{Subject to } g_j(X) \leqslant 0,\ j = 1, 2, \ldots J \\ &\qquad h_k(X) = 0\ k = 1, 2, \ldots K \\ &\qquad \min(X) \leqslant X \leqslant \max(X) \\ &\qquad X = [x_1, x_2, \ldots x_n] \end{aligned}$$

2. **Multiobjective cases**:

$$\begin{aligned} &\min \quad f_i(X),\ i = 1, 2, \ldots M \\ &\textit{Subject to } g_j(X) \leqslant 0,\ j = 1, 2, \ldots J \\ &\qquad h_k(X) = 0\ k = 1, 2, \ldots K \\ &\qquad \min(X) \leqslant X \leqslant \max(X) \\ &\qquad X = [x_1, x_2, \ldots x_n] \end{aligned}$$

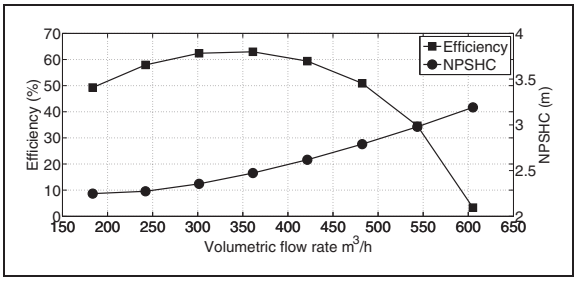

Figure 3. Total efficiency and NPSHC according to volumetric flow rate (reference machine). NPSHC: net positive suction head.

where M is the total number of objective functions, knowing that $M \geqslant 2$, $g_j(x)$ and $h_k(x)$ are the constraint functions of the inequality and the equality to be respected, with a total number J, K, respectively. In multiobjective problem, the solution is not unique, but a set of different nondominated solutions that form the optimal Pareto front. In the case of the minimization of all objective functions, the notion of dominance is written as follows

$$\ll a \, dominates \, b \gg \Leftrightarrow a \prec b \Leftrightarrow \begin{cases} \forall i \in \{1, 2, 3, \ldots, n_f\}, & f_i(a) \leqslant f_i(b) \\ \exists j \in \{1,2,3,\ldots, n_f\}, & f_j(a) < f_j(b) \end{cases} \quad (1)$$

Objective functions

*Consideration of a single function bi-objective: I*n our study, we will focus on the optimization of the overall efficiency as well as on the NPSHC cavitation criterion at the nominal point (Figure 3). These two objectives are combined and taken into account in a single global objective function F to be maximized or minimized, so as to maximize the function f_1 (efficiency), and to minimize f_2 (NPSHC) simultaneously. Knowing that the two main objectives considered functions are not on the same scale, a normalization procedure will be carried out.

*Taking into account three different forms of objective functions F: W*e propose in this framework three forms of objective functions F. In form 1, the objective function F will be expressed as follows[23]

$$\max F(f1, f2) = \alpha f1/\max(f1) - (1-\alpha) f2/\min(f2)$$
$$f1 = \eta(Qv_{nom}), f2 = NPSHC(Qv_{nom}) \quad (2)$$

Knowing that max ($f1$) and min ($f2$) are the maximum and minimum efficiency and NPSHC values at the operating point (nominal), respectively. These are obtained by a single-objective optimization of each of them separately. With α is a weighting factor equal to 0.5, giving the same level of targeting.

Form 2 will be based on the normalization of two objectives combined with a weighting factor of 0.5[24]

$$A = [f1 - \max(f1)/(\min(f1) - \max(f1))] \quad (3)$$

$$B = [f2 - \min(f2)/(\max(f2) - \min(f2))] \quad (4)$$

$$\max F(f1, f2) = \alpha(A) - (1-\alpha)(B) \quad (5)$$

In form 3, the objective is to minimize the Euclidean distance between the ideal point and the point of the solution provided by the used algorithm; the ideal point is the theoretical point which contains the two best optimized objectives separately, in our case it is $\max(f_1)$ and $\min(f_2)$.

With this form of objective function (equation (6)), we seek to bring the solution as close as possible to the ideal point. This approach is used in our work as a decision criterion in choosing one solution on the optimal Pareto front. In this technique, the normalization of objectives is primordial, where the objectives are normalized in interval of [0, 1], and the ideal point will have the coordinates (0, 0). Our goal will be to minimize the Euclidean distance between the ideal point and the solutions proposed by the CS algorithm (Figure 4)

$$\min F(f1, f2) = \sqrt{A^2 + B^2} \quad (6)$$

*Consideration of a multiobjective function: I*n this section, we consider the same objectives taken into account previously (efficiency and NPSHC). Contrary to the first strategy, the processing of the latter will be done separately

$$\min f_1 = -\eta(Qv_{nom}), \min f_2 = NPSHC(Qv_{nom}) \quad (7)$$

Decision variables

Each set of decision variables defines a solution or individual in a population, i.e. a given geometric configuration of a turbomachine design. During the optimization procedure, all the variables are of the real type, with the exception of the number of rotor blades which is considered to be an integer. The variables taken into account are given in Table 1.

Depending on the case, if some of these parameters are constant, they do not belong to the set of decision variables considered.

Considered constraints and handling techniques

The design of the turbomachines is done under conditions that must meet the requirements of the specification or the physical problem considered. These constraints can be classified in our study into

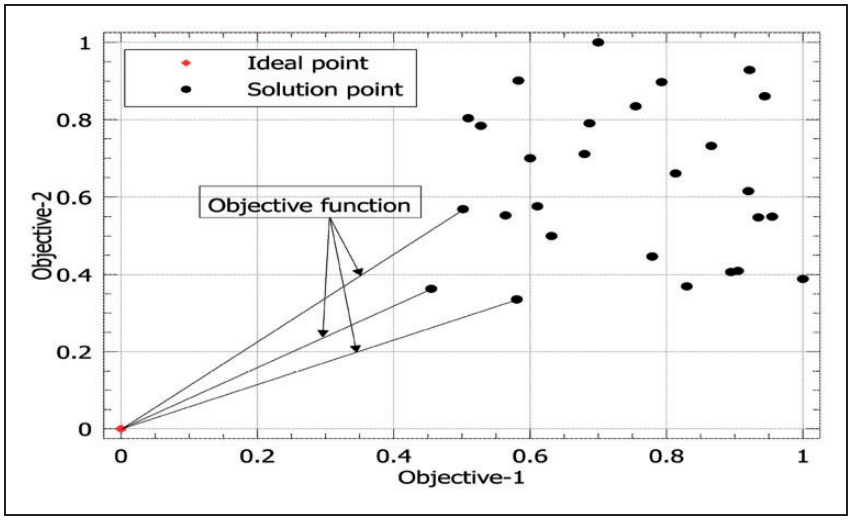

Figure 4. Proposed objective function in form 3.

Table 1. Decision variables considered.

Variable notation	Variable description
Qv	Initial theoretical volumetric flow rate
N	Rotational speed
R_i^1	The hub radius at the entrance of the rotor
R_e^1	The tip radius at the entrance of the rotor
R_e^2	The hub radius at the exit of the rotor
R_e^2	The tip radius at the exit of the rotor
D_i	Diffusion factor at the hub
D_e	Diffusion factor at the tip
Z	Number of rotor blades

three categories[20]:

1. **Side constraints**: The geometric optimization of the turbomachines requires the determination of the design space which consists of the min and max values of each variable. These adopted constraints are listed in the section of cases study.
2. **Geometric constraints**: The geometrical parameters of the profiles that describe the blade, namely: the chord, the stagger angle, the camber and the profile thickness, constitute the geometrical constraints to be respected. For empirical reasons related only to the NACA65 profile (flow stability, loss minimization, etc.), the camber was limited to a maximum value of 2.7. This constraint is expressed in each section as follows

$$C_{z\infty 0}^r - 2.7 \leqslant 0 \tag{8}$$

3. The same applies for the solidity at the entrance and the exit of the rotor

$$\sigma_1^r - 1.5 \leqslant 0 \text{ and } \sigma_2^r - 1.5 \leqslant 0 \tag{9}$$

4. A rotor thickness constraint which represents the axial distance between the entrance and the exit (the projections of the chords on the longitudinal axis) has been added for the reasons of space requirements of the machine. The latter must not exceed a certain value called max rotor thicknesses. This constraint is represented mathematically as follows

$$l_r \cos(\gamma_r) - th_{\max} \leqslant 0 \quad r = 1, 2, \ldots, N_{rd} \tag{10}$$

5. Knowing that l and γ represent the chord and the stagger angle at each section r, respectively. th_{max} is the maximum allowable thickness of the rotor and N_{rd} is the number of discretized sections, in this study, it is fixed as 20.
6. Furthermore, taking into account the stochastic effect of the optimization algorithms employed, the hub radius at the entrance of the rotor may have values greater than the hub radius at the exit. A constraint on these two radii must be added in order to avoid instability and disruption of the flow

$$R_i^1 - R_i^2 \leqslant 0 \tag{11}$$

7. To ensure geometric relevance and to avoid any kind of inadequate shape of the optimized rotor blade, a constraint on the flow angles must be respected. The inlet blade angle must be greater than the exit blade angle on all radially discretized sections between the hub and tip of the rotor. This constraint is given by

$$\beta_1^r - \beta_2^r > 0 \tag{12}$$

8. 3. **Mechanical constraint**: By designing the maximization of efficiency as an optimization objective, the design leads us to a very low nominal flow rate;

for this, a minimum value of the nominal flow must be imposed as the lower limit to be respected. This constraint is given by

$$Qv_{nom} - \widehat{Q_v} \geqslant 0 \tag{13}$$

With $\widehat{Q_v}$ is the minimum volumetric nominal flow allowed.

One of the simplest methods (used in this paper) for constraint handling is the penalization of individuals that reside in the area of infeasible solutions with a constant penalty.[18] The evaluation of the penalty function is based on the sum of the constraints violated. The penalty function for a maximization problem with m constraints is written as follows

$$f_p = F(X) - \sum_{i=1}^{m} C_i \delta_i$$
$$where \begin{cases} \delta_i = 1, \textit{ if constraint } i \textit{ is violated} \\ \delta_i = 0, \textit{ if constraint } i \textit{ is satisfied} \end{cases} \tag{14}$$

With f_p is the objective function penalized, F is the objective function not penalized, and C_i is the penalty constant.

In the case of a multiobjective optimization problem, K. Deb[19] shows that the choice of the penalty factor is not an easy task. In the case of minimization of multiobjective functions, for low penalty factor values (0.01, 0.1, 0.5, and 1) Pareto front resides on the infeasible area. With a penalty factor of 10, the pseudo-front is very close to the exact Pareto front; with a value of 100, the solutions distribution is not well spreaded as those with the previous penalty factor value.

A different approach was proposed,[25] which consists of using the so-called constrained-domination. The basic concept underlying this approach is straightforward: a solution a is said to constrained-dominate a solution b if any of the following conditions is true:

1. Solution a is feasible and solution b is not.
2. Solutions a and b are both infeasible, but a has a smaller overall constraint violation.
3. Solutions a and b are both feasible and a dominates b.

Bio-inspired algorithms for solving optimization problems

CS algorithm (basic version)

During the last decade, the newly developed nature-inspired algorithms have attracted much attention of researchers and have also been widely applied to optimization problems. Among these algorithms that proved its effectiveness, we will mention: the CS, it is mainly based on the parasitism of the cuckoo in the brood phase. Some types of this bird lay their eggs in a nest of other individuals instead of building a nest. This idea has been coupled with Levy flight[26,27] that represents the behavior of some birds and fruit flies, mathematically called random walk, with a length of step taken from the distribution of Levy according to natural inspired.[28] By analogy, the host nest represents an individual and the eggs are represented by the decision variables.

The CS algorithm is principally based on three phases:

1. The get nest phase: each cuckoo lays one egg at a time in a randomly chosen nest (equations (15) to (21))

$$x_i^{(t+1)} = x_i^{(t)} + \alpha \oplus L\acute{e}vy(\beta) \tag{15}$$

$$\alpha = \alpha_0 \times (best - x_i^{(t)}) \tag{16}$$

$$\alpha_0 \times (best - x_i^{(t)}) \oplus L\acute{e}vy(\beta) \approx 0.01 \frac{\mu}{|v|^{\frac{1}{\beta}}} \left(best - x_i^{(t)}\right) \tag{17}$$

$$\mu \approx N(0, \sigma_\mu^2) \tag{18}$$

$$v \approx N(0, \sigma_v^2) \tag{19}$$

$$\sigma_\mu = \left[\frac{(\Gamma(1+\beta)\sin(\beta\pi/2))}{(\Gamma[(1+\beta)/2] \times \beta \times 2^{(\beta-1)/2})}\right]^{\frac{1}{\beta}} \tag{20}$$

$$\sigma_v = 1 \tag{21}$$

where μ is the normal distribution of an average of 0 and a variance of σ_μ^2, and v is the normal distribution of an average of 0 and a variance of 1.

2. The best nest phase: after the comparison between the new and old individual, the best nest with good quality eggs will be chosen for the next generation.
3. The empty nest phase: with a probability of pa, the egg laid by the cuckoo can be discovered by the host bird. In this case, the host bird can dump the egg or abandon completely the nest and construct another. The phase of changing the nest for the aim of finding a new solution with biased/selective random walks[26] is given as follows (equations (22) and (23)).

Two solutions x_p, x_q are randomly selected, and a new nest from these two solutions is then looked for, therefore

$$stepsize = rand \times (x_p^t - x_q^t) \tag{22}$$

$$new\_x_i^t = x_i^t + stepsize \tag{23}$$

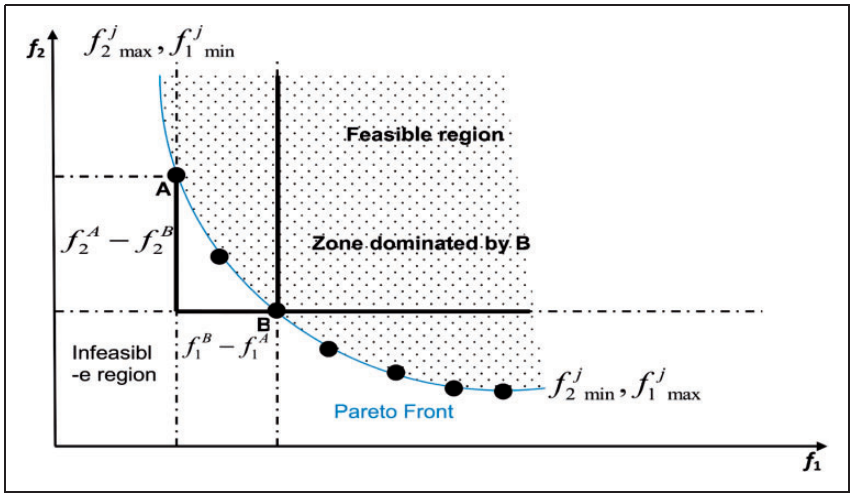

Figure 5. Pareto front and crowding distance.

NSCS algorithm

After proving to be efficient and fast and cost-effective for solving single-objective problems, the CS metaheuristic optimization algorithm has been extended to the multiobjective version by Yang and Deb.[29] This version has been used to solve various problems; for further information and a more in-depth analysis of the diverse applications, the reader may refer to Wang et al.,[30] Rani et al.,[31] and Fister et al.[32] The NSCS was developed by He et al.[33]

According to Deb et al.,[25] each solution must be compared to the entire population, in order to determine if it is dominated by another solution. Then, a sorting by fronts is done in the following order: the first front contains the solutions that are nondominated by other solutions. The second front is constructed by the set of solutions dominated only by the individuals of the first front. The third front is composed by the set of solutions that are dominated by the first and the second fronts, and so on, until all individuals of the population will be sorted and classified. At the front, the classification of solutions by the dominance does not ensure a uniform density, which is one of the disadvantages of the aggregation scheme method. For this reason, another technique called the crowding distance (Figure 5) is adopted to evaluate the local aggregation. The principle of this technique consists of classifying the solutions of the same front according to their objectives. The two extreme points (Min, Max) take an infinite distance. The crowding distance of the intermediate points is then computed as the ratio between the distance of the two neighborhood objectives and the distance of the two extremes. The crowding distance is written as the following equation

$$C_j = \sum_{i=1}^{Nobj} \frac{F_i^{j+1} - F_i^{j-1}}{(F_i^j)_{\max} - (F_i^j)_{\min}} \tag{24}$$

In fact, the main idea of crowding distance calculation is to find the Euclidean distance between the solutions (individuals) in a front to obtain uniform distribution solution points, which makes solutions that have a greater distance more favored. On each of the resultant fronts, solutions are ranked according to their distances in descending order, such as

$$\begin{aligned} a \prec b \Leftrightarrow \{&a_{rank} < b_{rank} \text{ or } ((a_{rank} = b_{rank}) \\ &\text{and } (a_{distance} > b_{distance}))\} \end{aligned} \tag{25}$$

Now we briefly describe the optimization processing procedure using the NSCS algorithm, which is almost similar to the NSAGII algorithm.[25] A population P of size N is generated randomly. Another population Q of the same size will be constructed from the first one according to the "get nest" and "empty nest" phases. Then, a population R with size of $2N$ will be generated by combination of P and Q, whose individuals are classified according to the notion of the dominance constraint according to expression (25). After that, the individuals of the same front are sorted by the crowding distance (equation (24)). Finally, the new population P of size N is generated containing the individuals that have a good front's rank with a greater distance.

In order to examine the quality of the optimum front obtained by the optimization algorithms, particular measurement techniques are employed[25,34,35] and they are also used in NSCS[33]:

1. **Index of convergence *Ic***: represents the average normal distance between the obtained Pareto front (all the points) and exact Pareto front. The normal distance of a solution is the closest one to the true Pareto front.
2. **Index of diversity *Id***: it is used to measure the distribution level of the points on the Pareto front

according to the following equation

$$Id = \frac{1}{M}\sum_{k=1}^{M}\frac{f_k(z_k^{\max}) - f_k(z_k^{\min})}{f_k^{\max} - f_k^{\min}} \tag{26}$$

3. With M is the number of objective functions; $z_k^{\max}$ and $z_k^{\min}$ are the maximum and minimum values of the kth objective, respectively; $f_k^{\max}$ and $f_k^{\min}$ are the coordinates of objectives k in the two extremes of the front.
4. **Uniformity index *Iu***: it measures the uniformity of the solutions distribution on the front, expressed by the variance of the Euclidean distances (crowding distance)

$$Iu = \mathrm{Var}[D_N] \tag{27}$$

Where

$$D_N = \sqrt{\sum_{k=1}^{M}\frac{f_k(a) - f_k(b)}{f_k^{\max} - f_k^{\min}}} \tag{28}$$

For a good performance, *Ic* and *Iu* should be close to 0 and *Id* should be close to 1.

Test functions for implementing optimization algorithms

To prove the effectiveness of the used algorithms, three benchmark functions were tested for both types of optimization problems, i.e. single objective and multi-objective, for the first one: the Rosenbrock's function (Fun 1)[36] is written as follows

$$f(x) = \sum_{i=1}^{N-1}\left[100(x_{i+1} - x_i^2)^2 + (1 - x_i)^2\right] \tag{29}$$

where N is the number of variables, and $-5 \leqslant x_i \leqslant 5$. The global minimum of this function is $f(x) = 0$ at the solution of $x = (1, 1 \ldots 1)$.

The second function is known as sphere function (Fun 2) and is given by

$$f(x) = \sum_{i=1}^{N} x_i^2 \tag{30}$$

with $-100 \leqslant x_i \leqslant 100$, its global minimum resides in $x = (0, 0 \ldots 0)$, and $f(x) = 0$.

The last function for single objective test is Schwefel's function (Fun 3)[37]; it is a multi-modal function whose global minimal $f(x) = 0$ at $x = (420.9687, 420.9687, \ldots, 420.9687)$ according to the following form

$$f(x) = 418.982887274338N - \sum_{i=1}^{N} x_i \sin(\sqrt{|x_i|}) \tag{31}$$

where $-500 \leqslant x_i \leqslant 500$.

For multiobjective: Schaffer's function (SCH)[38] was chosen as first function test and it is written as

$$\text{Minimize} = \begin{cases} f_1(x) = x^2 \\ f_2(x) = (x-2)^2 \end{cases} \quad -10^3 \leqslant x \leqslant 10^3 \tag{32}$$

The second one is so-called FON[39] and can be presented as follows

$$\text{Minimize} = \begin{cases} f_1(\mathbf{x}) = 1 - \exp\left[-\sum_{i=1}^{n}\left(x_i - \frac{1}{\sqrt{N}}\right)^2\right] \\ f_2(\mathbf{x}) = 1 - \exp\left[-\sum_{i=1}^{n}\left(x_i + \frac{1}{\sqrt{N}}\right)^2\right] \end{cases} \quad -4 \leqslant x_i \leqslant 4,\ 1 \leqslant i \leqslant N \tag{33}$$

The last function is a constraint example (CONSTR)[19]

$$\text{Minimize} = \begin{cases} f_1(x_1, x_2) = x_1 \\ f_2(x_1, x_2) = \frac{1+x_2}{x_1} \end{cases} \quad \text{subject to} \begin{cases} g_1(x_1, x_2) = x_2 + 9x_1 \geqslant 6 \\ g_1(x_1, x_2) = -x_2 + 9x_1 \geqslant 1 \end{cases} \quad 0.1 \leqslant x_1 \leqslant 1, 0 \leqslant x_2 \leqslant 5 \tag{34}$$

The employed GA is based on real coded with a binary crossover and polynomial mutation.[40] For the reproduction operation, the binary tournament selection was chosen. For all functions $N = 3$, and the program's execution was repeated for 50 runs with 100,000 function evaluations for each run. Since the comparison between CS and Ga was studied,[27] the goal of this test is not the comparison, but for giving more credibility to the implementing algorithms and support subsequent conclusions. From Figure 6 and Tables 2 and 3, we can note a very acceptable and close result between the methods with a little superiority of CS.

Cases study: Optimization of mono-rotor pump design

*Technical specifications: T*he following technical specifications are based on the data of the adopted reference pump and are summarized in Table 4. Other specifications that are directly related to the design must be laid down and kept constant during all the optimization steps and for the two cases of the study (Tables 5 and 6).

*Development of objective functions and pseudo-code implemented. Single bi-objective function: T*he CS algorithm, like all metaheuristic algorithms, requires

several evaluations of objective function to determine the optimal solution. Consequently, a stopping criterion limiting the maximum number of iterations to 300, with a population size of 100, and a probability of 0.25 of abandonment and nest change is imposed. Many runs are repeated for choosing the best solution. The pseudo-code of Algorithm 1 illustrates the incorporating strategy of the CS algorithm within the inverse design. As mentioned in the previous sections, for the first case, the decision variables and their side constraints are summarized in Table 6. According to the mono-objective optimization carried out previously (Figure 7(a) to (d)), form 1 of the global objective function for this first case becomes

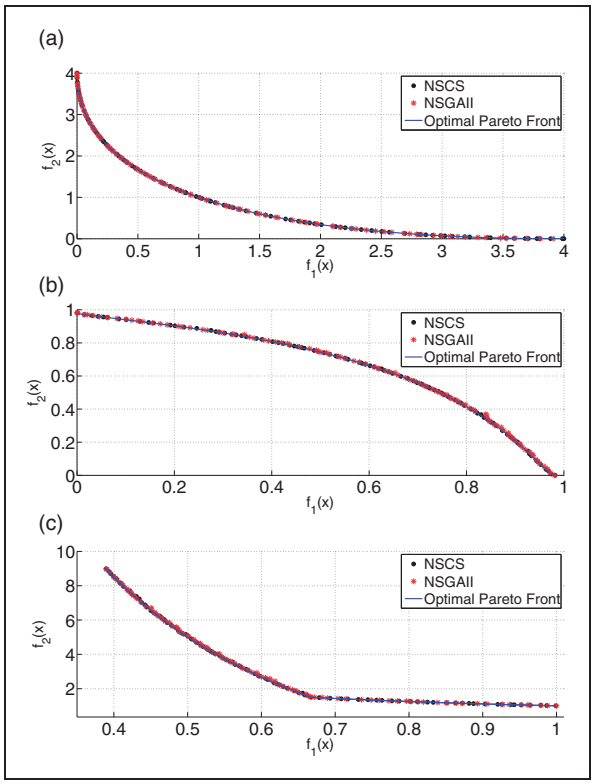

Figure 6. Comparison between the true Pareto front, NSCS, and NSGAII. (a) SCH, (b) FON, and (c) CONSTR. NSCS: nondominated sorting cuckoo search; NSGAII: nondominated sorting genetic algorithm.

$$\max \; F = f_1/0.7384 - f_2/1.5600 \tag{35}$$

For form 2

$$A_1 = (f_1 - 0.7383)/(0.7067 - 0.7383) \tag{36}$$

$$B_1 = (f_2 - 1.5600)/(2.1671 - 1.5600) \tag{37}$$

$$\min F = \alpha A_1 + (1-\alpha)B_1 \tag{38}$$

Table 4. Specifications of the reference pump.

Parameters	Axial pump
H (m)	1
Q (m^3/h)	472.5
N (r/min)	840
Q min (m^3/h)	180
Q max (m^3/h)	1800

Table 2. Comparison of CS with GA in single-objective optimization.

	CS				GA			
Function	Min	Max	Mean	Std	Min	Max	Mean	Std
Fun 1	0	0	0	0	8.1282e-09	0.0107	3.7512e-04	0.0017
Fun 2	0	0	0	0	0	0	0	0
Fun 3	5.712536e-09	5.712536e-09	5.712536e-09	0	5.712536e-09	5.712536e-09	5.712536e-09	0

CS: cuckoo search; GA: genetic algorithm.

Table 3. Comparison of CS with GA in multiobjective optimization.

	CS			GA		
Function	*Ic*	*Id*	*Iu*	*Ic*	*Id*	*Iu*
SCH	0.008	1.0000	0.0059	0.0078	0.9996	0.0060
FON	0.0012	0.9999	0.0035	0.0023	1.0006	0.0038
CONSTR	0.0054	0.9998	0.0057	0.0056	1.0012	0.0060

CS: cuckoo search; GA: genetic algorithm.

and for form 3

$$\min F = \sqrt{A_1^2 + B_1^2} \tag{39}$$

Table 5. Theoretical specifications.

Theoretical parameters	Axial flow pump
Vortex	Forced
Density of fluid (kg/m^3)	1000
Clearance (m)	5.0e-4
Roughness of rotor (m)	2.0e-5
Number of volumetric flow rate	30
Number of section	25
Radial equilibrium	Simplified
Maximum blade thickness	0.012

Table 6. Side constraint and specifications of the two cases.

Objective max(η_{nom})/ min($NPSHC_{nom}$)		
Case	1	2
N (r/min)	[840.00]	[400.00, 1000.00]
Q_v(m^3/h)	[180.00, 1800.00]	[472.5]
R_i^1(m)	[0.03, 0.100]	[0.04]
R_e^1(m)	[0.105, 0.150]	[0.105, 0.150]
R_i^2(m)	[0.03, 0.100]	[0.04]
R_e^2(m)	[0.105, 0.150]	[0.105, 0.150]
D_i	[0.3, 0.7]	[0.3, 0.7]
D_e	[0.3, 0.7]	[0.3, 0.7]
Z	[3, 10]	[3, 10]

In the second case, during the optimization, the volumetric flow rate and the hub radius are fixed as those of the reference machine, and the decision variables are taken from Table 6.

According to the mono-objective optimization carried out (Figure 7(a) to (d)), form 1 of the global objective function becomes in this second case

$$\max F = f_1/0.71209 - f_2/1.56842 \tag{40}$$

for form 2

$$A_2 = (f_1 - 0.712)/(0.7075 - 0.712) \tag{41}$$

$$B_2 = (f_2 - 1.568)/(1.687 - 1.568) \tag{42}$$

$$\min F = \alpha A_2 + (1-\alpha)B_2 \tag{43}$$

And for form 3

$$\min F = \sqrt{A_2^2 + B_2^2} \tag{44}$$

Algorithm 1: Optimization of axial flow pump design by CS

```
begin
    Read the input parameters
    Initialize the population randomly
    Evaluate the population by:
        1- Inverse design
        2- Performance analysis
        3- Computation of objective function, constraint
       checking and fitness calculation
    for iteration=1 to Max iteration do
        Generate new solution by get nest phase
        Evaluate the population by:
            1- Inverse design
            2- Performance analysis
            3- Computation of objective function,
           constraint checking and fitness calculation
        Keeping the best solutions
        Generate new solution by empty nest phase
        Evaluate the population by:
            1- Inverse design
            2- Performance analysis
            3- Computation of objective function,
           constraint checking and fitness calculation
        Keeping the best solutions
    end
    return Best solution
end
```

*Multiobjective functions: T*he proposed optimization approach consists of minimizing the objective functions f_1 and f_2 simultaneously, with the goal of maximizing the efficiency and minimizing the NPSHC at the nominal point, such that

$$f_1 = -\eta(Qv_{nom}) \; and \; f_2 = NPSHC(Qv_{nom}) \tag{45}$$

The variable specifications employed in the two cases above remain the same for this case.

The pseudo-code Algorithm 2 describes the inverse design of an axial pump with NSCS.

There is no unique optimal solution but rather, a set of solutions forming an optimal Pareto front. Since only one point should be chosen, we consider the optimum, which is the closest solution to the ideal point[41] that it is the optimal solution of each objective function from a mono-objective. In other words, this point represents the two best optimas in the Pareto front. On the other hand, the nadir point is the intersection of the two furthest positions from the solutions of the optimum front. Several researches have tackled the challenge reaching this point by optimizing each objective individually.[42–44] The ideal/nadir points are used in this work for the normalization of the objectives. Thus, each objective function is replaced by a normalized function[24,45] (equation (46)), in order to find the nearest ideal point solution, based on the minimal Euclidean distance

$$0 \leqslant \frac{f_i(x) - z_i^U}{z_i^N - z_i^U} \leqslant 1, \quad \forall i = 1, \ldots, k \tag{46}$$

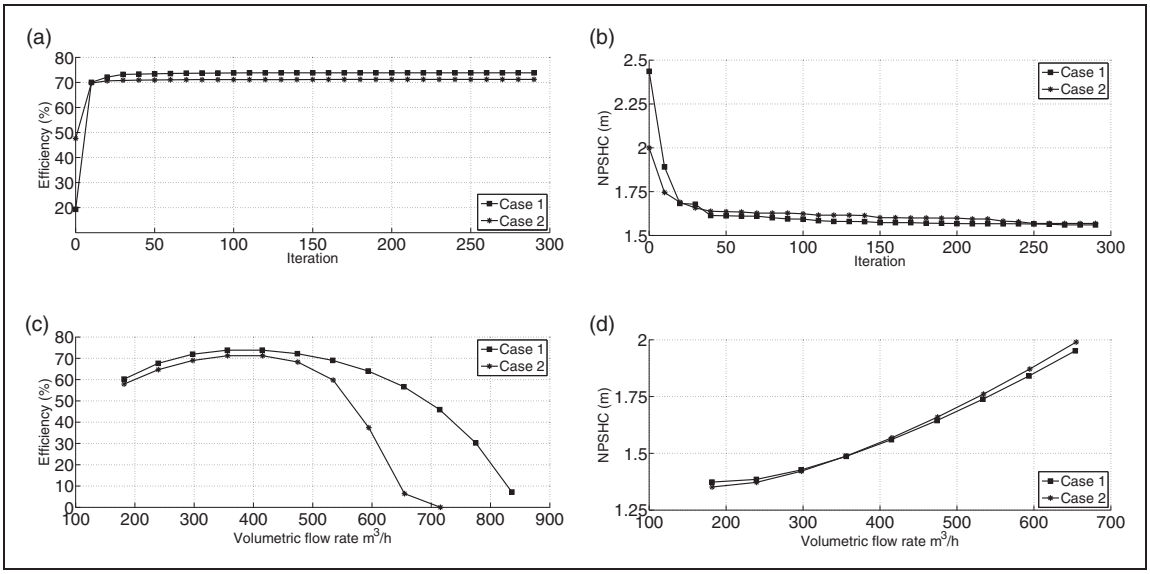

Figure 7. Optimization of two objectives separately. (a) Evolution of total efficiency with iteration, (b) evolution of the NPSHC with iteration, (c) evolution of total efficiency with volumetric flow rate, and (d) evolution of the NPSHC with volumetric flow rate.

With z_i^U: the ideal point component and z_i^N: the nadir point component.

Algorithm 2: Optimization of axial flow pump design by NSCS

```
begin
    Read the input parameters
    Initialize the population P of size N randomly
    Evaluate P by:
        1- Inverse design
        2- Performance analysis
        3- Computation of objective functions, constraint
       checking
    Sort solution P by non-dominated technique and
     crowding distance
    for iteration=1 to Max iteration do
        Generate new solution Q of size N by CS
         (phases get nest and empty nest)
        Evaluate Q by:
            1- Inverse design
            2- Performance analysis
            3- Computation of objective functions,
           constraint checking
        R=P ∪ Q
        Sort R by non-dominated technique
        Generate population P of size N from R by the
         crowding distance classification for each front
    end
    return P
    Tracing Pareto front
end
```

Results and discussion

Case one

In the first case, considered variables are represented in Table 6, and the rest of the variables are the same as the reference pump.

*Evolution of the objective functions and variation of the optimal Pareto front as a function of population size: I*n the case of form 1 of the objective function, Figure 8(a) shows the monotonic evolution of both objective functions, maximizing the efficiency and minimizing the NPSHC. This is not the case for the other forms (shown in Figure 8(b) and (c)), where the efficiency and NPSHC curves follow a nonmonotonic pattern, characterized by a peak at the beginning of the iterative process. We note that from the 50th iteration, the improvement of fitness is negligible compared to the first 50 iterations.

Figure 9(a) shows the variation of the Pareto front for various population sizes. First, we can observe that all front curves came closer from each other. Second, because of its uniformity, the front related to the 600 individual cases is chosen as a benchmark example. With 600 individuals and at 100 iterations, the front begins to take the shape of the optimal front and the next iterations are for improving the precision and the distribution points (Figure 9(b)). Figure 9(c) confirms that the optimal front contains only the non-dominated solutions. The far points represent the fronts of the first iterations. In Figure 9(d), the uniformity and diversity of the front curves are explicitly highlighted. We also find that the reference point is very far from this optimal front, thus exceeding the nadir point. Figure 9(e) illustrates the distribution of the optimized performance of the machine considered on the optimal Pareto front:

- In the case of a single objective function of form 1, NPSHC is more preponderant compared to the total efficiency; the value of the weighting coefficient $\alpha = 0.5$ is not respected. The Pareto front constructed by this objective function has a high

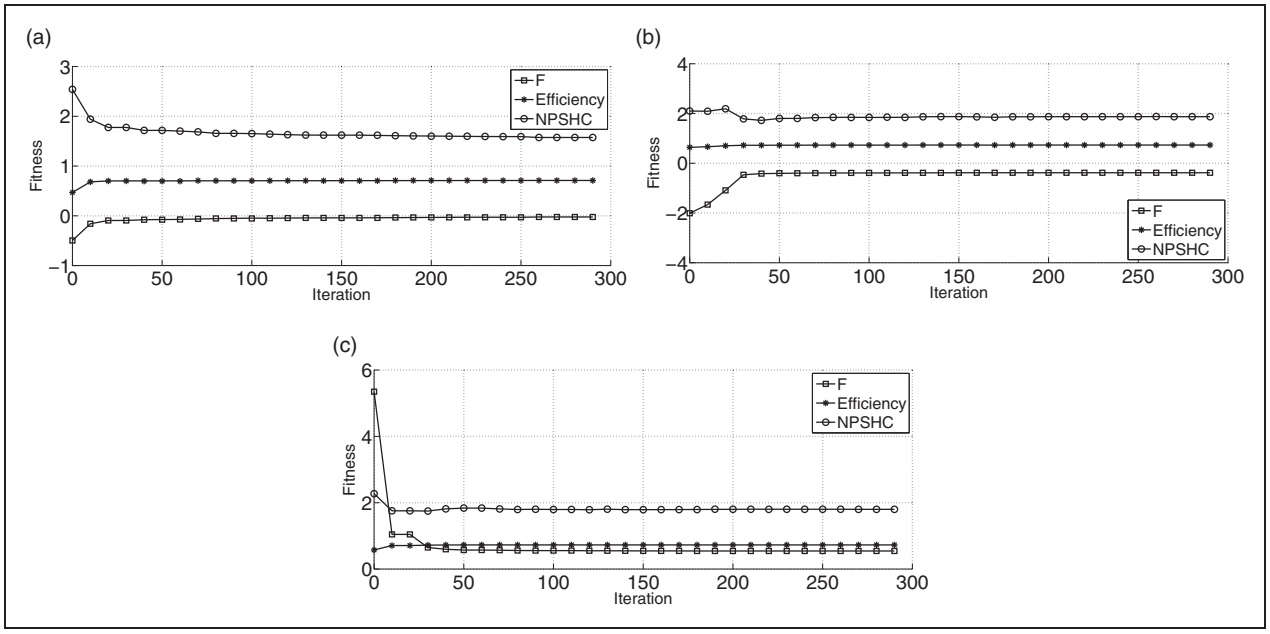

Figure 8. Evolution of global objective function with iteration: case 1. (a) Form 1, (b) form 2, and (c) form 3. NPSHC: net positive suction head.

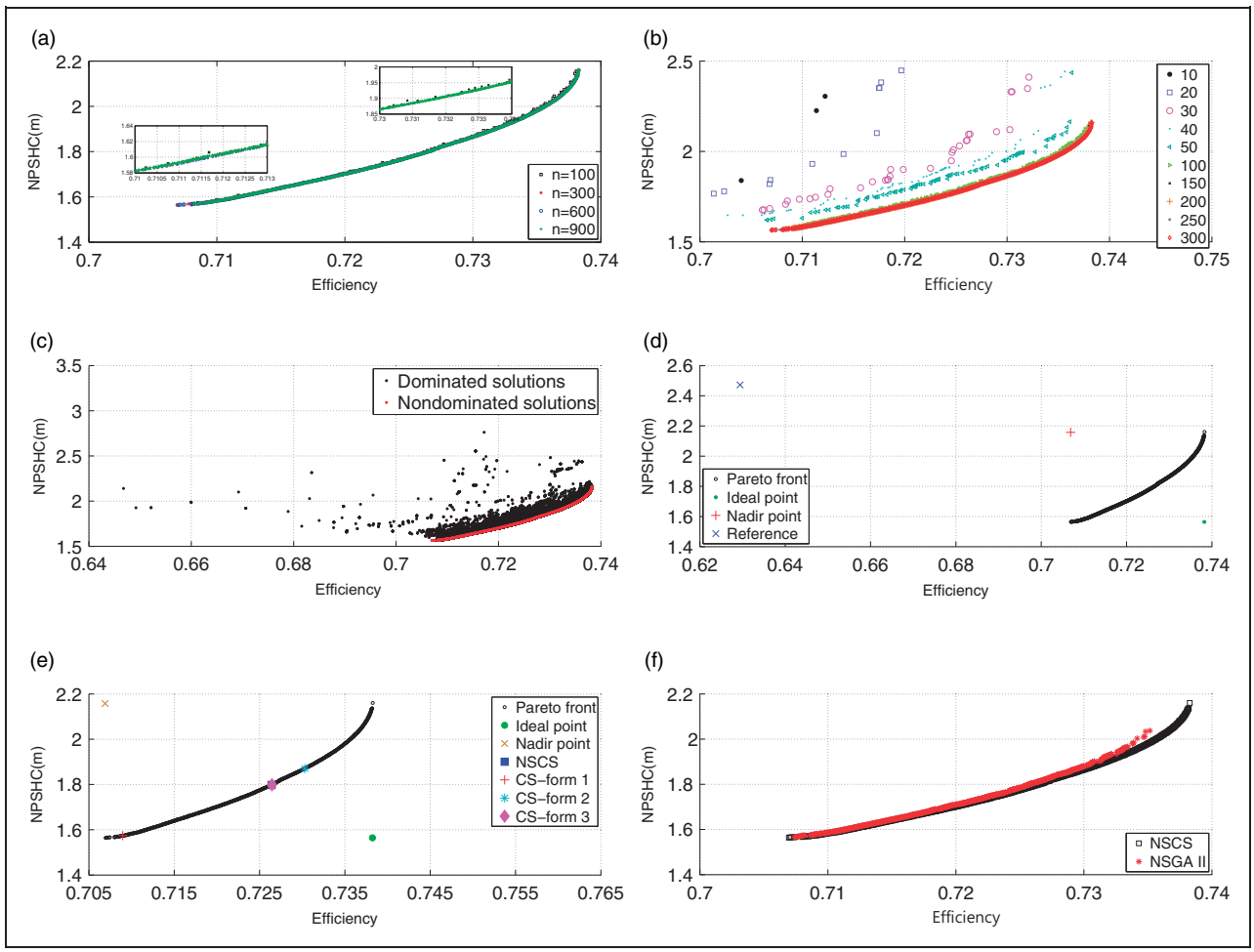

Figure 9. Pareto front and optimized points: case 1. (a) Evolution of the optimal front with population size, (b) evolution of the optimal Pareto front during the loop (n = 600), (c) nondominated solution versus dominated solutions (overall iterations with n = 600), (d) comparison of reference machine and optimal front (n = 600), (e) comparison of overall optimal solution with Pareto front of population size n = 600, *Id* = 1.0137, *Iu* = 1.8890e-04, and (f) NSCS versus NSGAII with a population of 600 individuals. CS: cuckoo search; NPSHC: net positive suction head; NSCS: nondominated sorting cuckoo search; NSGAII: nondominated sorting genetic algorithm.

probability to be poorly distributed with a reduced diversity. Therefore, a lower $\Delta\alpha$ value in this case can considerably increase the computational time.
- In the case of form 2 of the objective function, the adopted approach shows a better ability to construct an optimal front than the previous form.
- In the case of form 3, the aim is to minimize the distance between the solution provided by the cuckoo algorithm and the ideal point. The obtained solution is approximately identical to the solution chosen in the NSCS approach that shows that it is effective providing satisfactory measurements of the diversity and uniformity indices.

Although the NSGAII provides good results in benchmark test functions, it is not the case with optimization of the axial flow pump design. Figure 9(f) shows its inability to provide an optimal front. On the contrary, NSCS is proven to be more effective convergence in terms of uniformity or diversity. NSGAII for this kind of problem, with a large decision variables and constraints, may need more evaluations and adjustment of the control parameters which remains undesirable in optimization domain.

*Configurations of the optimal machines: T*able 7 shows the overall results. For bi-objective optimization, taking into account a single objective function, we observe that:

- In form 1, the efficiency and NPSHC are improved by 12.63 and 36.48%, respectively.
- In form 2, the efficiency and NPSHC are improved by 16.03 and 24.35%, respectively.
- In form 3, the efficiency and NPSHC are improved by 15.42 and 27.26% respectively. We find that adopting this form gives identical results to the NSCS-based approach (15.42 and 27.26%).

The decision variables for all optimized pump designs are based on hub radius values at the lower limit of the search interval. On the other hand, for tip radius, it was preferable to choose values at the upper limit of the search space. In other words, the optimized pump designs have very low hub/tip ratios. For the diffusion factor, the solutions obtained look like a constant vortex, with high values at the hub and on the tip of the blade, despite the choice of a forced vortex in accordance with the reference machine that has a factor of reduced diffusion at the hub of the blade. Furthermore, because of the limitation of the operating flow range, corresponding to a height H of 1 m, the volumetric flow rates are close to the reference one. The number of blades converged to 3 in all the scenarios studied.

The geometry of the reference and optimized pump (with NSCS) is presented in Figure 10. We clearly distinguish two points of comparison: the first one is the hub/tip ratio, the reference rotor (Figure 10(a)) has greater value compared to the optimized one

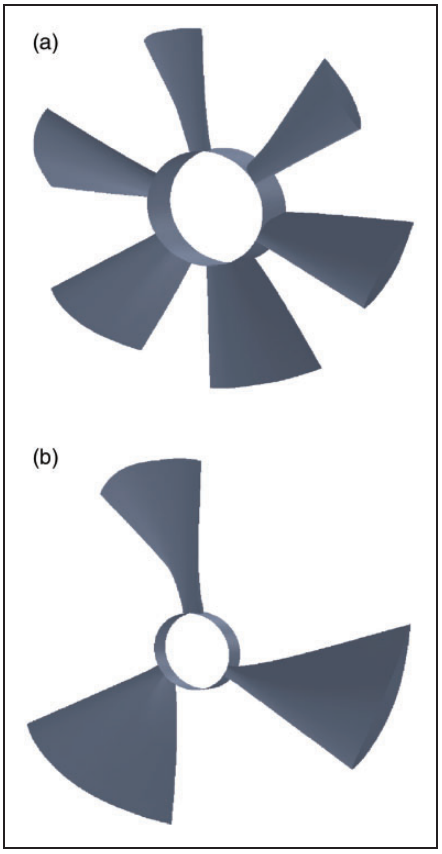

Figure 10. Case 1: reference rotor CAD versus optimal rotor CAD (NSCS). (a) Reference rotor CAD and (b) optimal rotor CAD.

(Figure 10(b)); the second one is the axial rotor thickness (constraint in Equation (10)) which it is respected in the optimized pump.

*Evolution of machines' performances as a function of volumetric flow rate: T*he evolution of the performances of the optimized pumps is presented in Figure 11. Figure 11(a) highlights the improvement of the efficiency in relation to the optimized machines' design. We note that in addition of the higher efficiency and lower NPSHC, in cases of objective functions of form 2, 3 and NSCS, there is an improvement of the results by including a wider range of operations for high efficiency where the flow rate varies between 180 and 690 m^3/h. The results obtained for the height H (not considered as an objective function) are shown in Figure 11(b), which indicate an increase over the entire range of variations relative to the reference machine. It is also observed that the difference between the nominal points of the optimized pumps is not very obvious.

Figure 11(c) and (d) represents the variation of NPSH and NPSHC, respectively. We clearly observe that the results obtained from form 1 of objective function favor the NPSHC comparatively with objective functions of the form 2 and 3. The difference between the optimized pumps and the reference pump is quite clear. In addition, all resulting pump

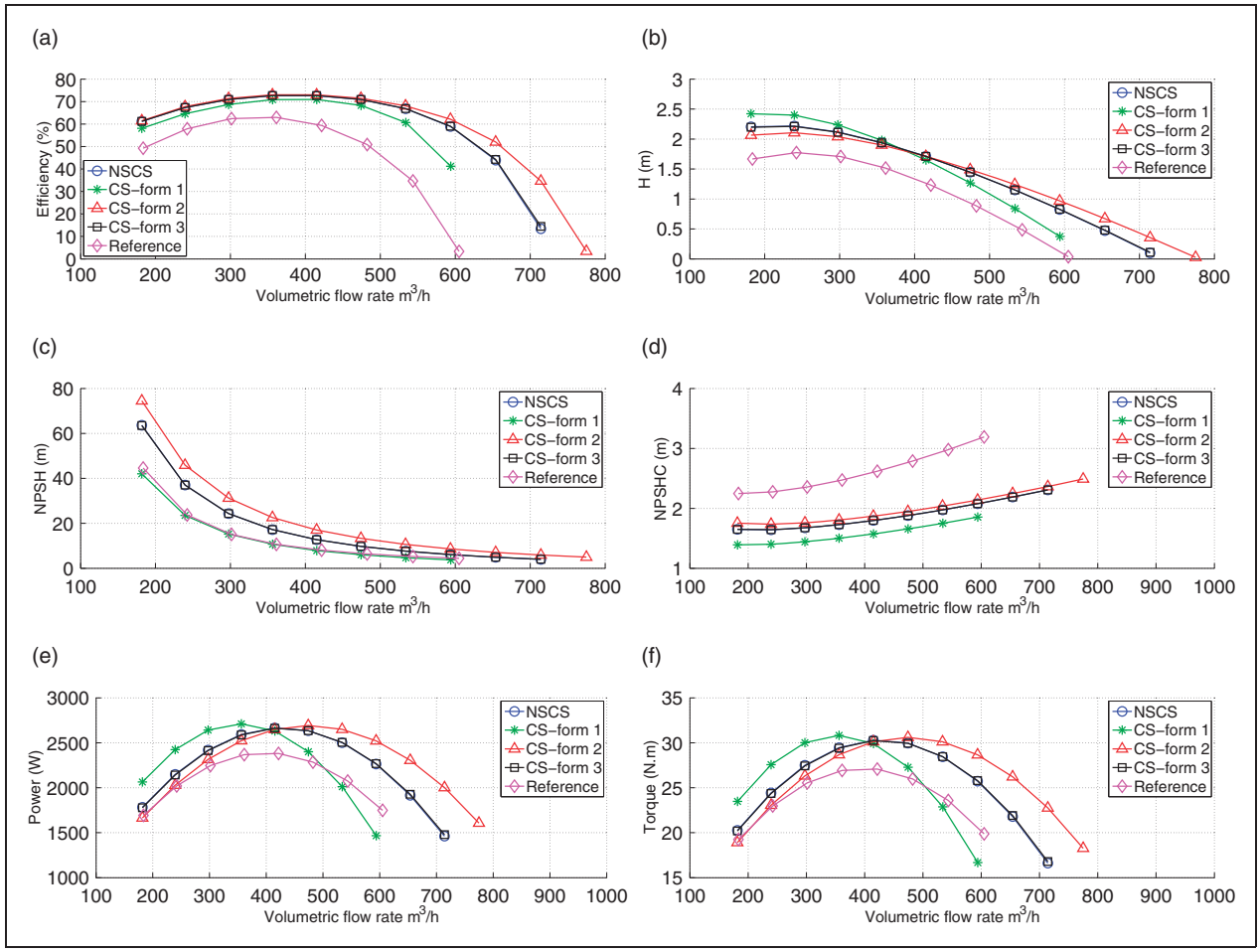

Figure 11. Case 1: performances. (a) Evolution of total efficiency, (b) evolution of the head, (c) evolution of the NPSH, (d) evolution of the NPSHC, (e) evolution of the power, and (f) evolution of the torque. CS: cuckoo search; NSCS: nondominated sorting cuckoo search.

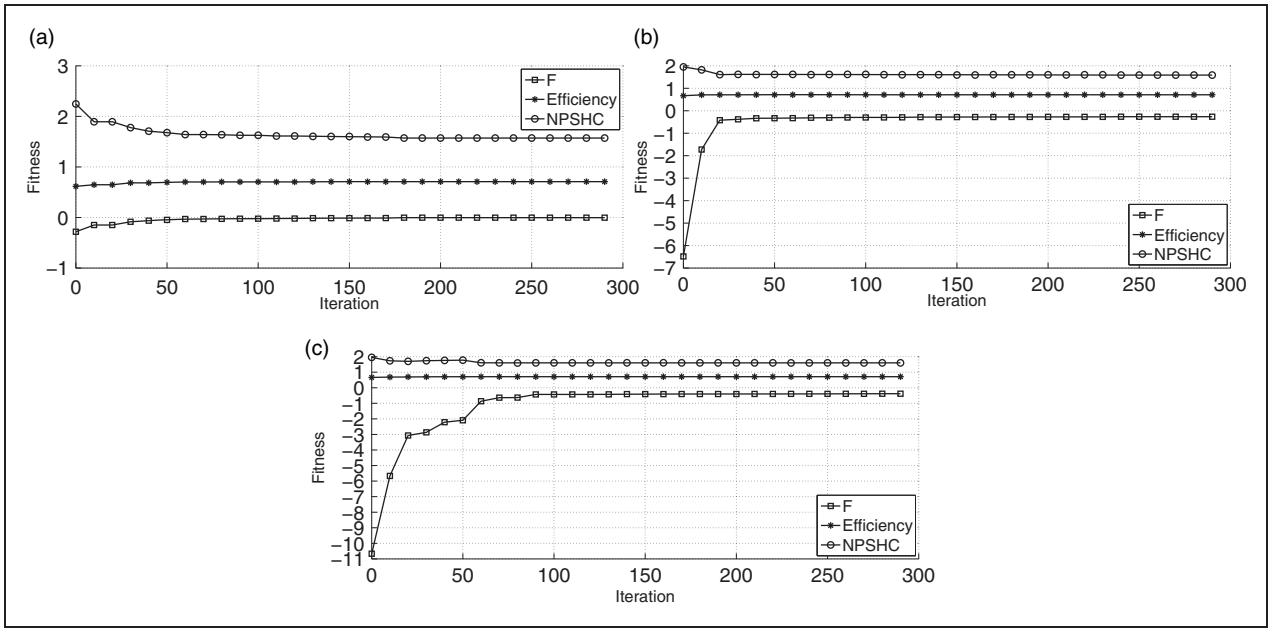

Figure 12. Evolution of global objective function with iteration: case 2. (a) Form 1, (b) form 2, and (c) form 3. NPSHC: net positive suction head.

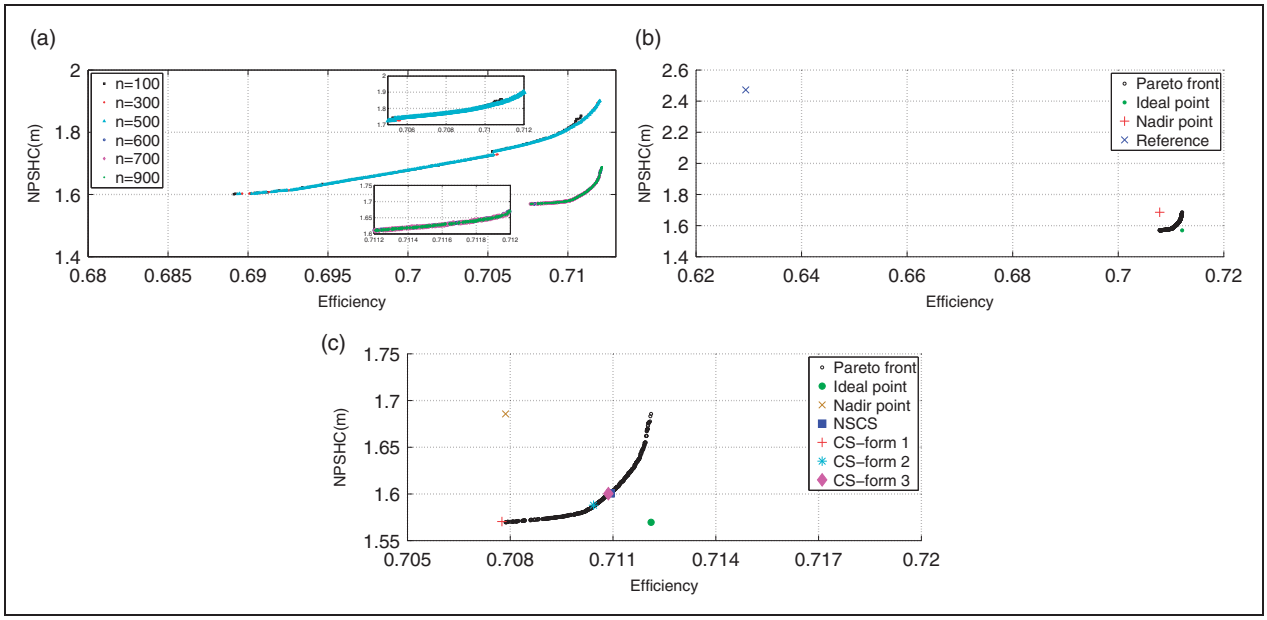

Figure 13. Pareto front and optimized points: case 2. (a) Evolution of the optimal front with population size, (b) comparison of reference machine and optimal front (n = 600), and (c) comparison of overall optimal solution with Pareto front population n = 600, *Id* = 1.05, *Iu* = 9.2252e-04. CS: cuckoo search; NPSHC: net positive suction head; NSCS: nondominated sorting cuckoo search.

designs have higher suction capacity than the reference machine, except the one optimized by the form 1, which exhibits identical variation of the NPSH.

In Figure 11(e) and (f), where the shaft power and torque are considered, we observe that the optimized pumps consume more energy than the reference one, with a consumption gap of about 12%. We also observe the existence of an intersection point between the optimized pumps located approximately in the vicinity of the nominal point. Finally, based on the results shown in Figure 11, we can conclude that the objective function for the minimization of the distance between the optimal solution and the ideal point gives the same results compared to the solution chosen from the optimal Pareto front, and the performance curves confirm this fact very clearly.

Case two

In this case, the flow rate and the hub radius are considered as constants, while the rotational speed, the tip radius, the diffusion factors, and the number of blade rotors are taken as decision variables.

*Evolution of the objective functions and variation of the optimal front of Pareto according to the population size: F*igure 12 shows the evolution of the objective function and their fitness as a function of the number of iterations. In comparison with case 1, the convergence in case 2 requires greater number of iterations. This can be explained by the fact that in this case we consider a large range of rotational speed. Figure 13(a) shows that from certain population size (600 individuals) the Pareto front reaches its optimal

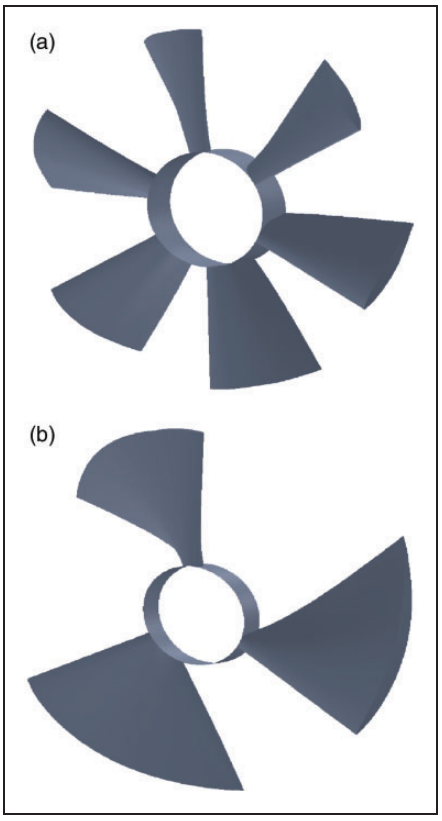

Figure 14. Case 2: reference rotor CAD versus optimal rotor CAD (NSCS). (a) Reference rotor CAD and (b) optimal rotor CAD.

shape, which is also due to the increased rotational speed constraint side. In Figure 13(b), we notice a large difference between the reference pump and optimized pumps at the Pareto front. Figure 13(c)

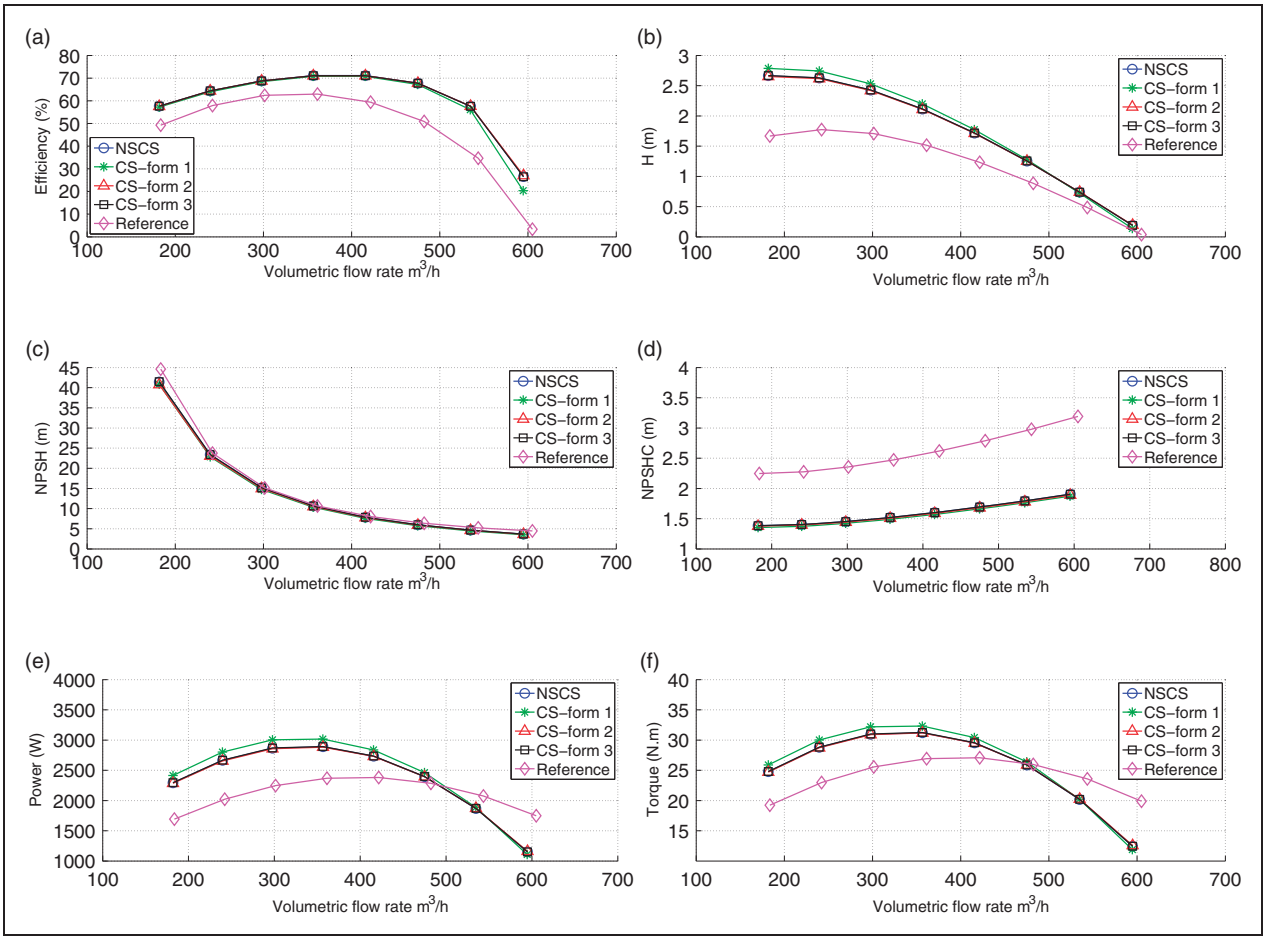

Figure 15. Case 2: performances. (a) Evolution of total efficiency, (b) evolution of the head, (c) evolution of the NPSH, (d) evolution of the NPSHC, (e) evolution of the power, and (f) evolution of the torque. CS: cuckoo search; NPSHC: net positive suction head; NSCS: nondominated sorting cuckoo search.

indicates that the solution obtained by the CS approach of form 1 does not belong to the Pareto front. The two solutions closest to the ideal point are not really confused but rather adjacent. The optimization process would need more iterations to improve the convergence. Concerning form 2 of the objective function, the solution obtained is very close to the Pareto front, and therefore remains acceptable.

It is also seen, in Figure 13(c), that in this case, the index of diversity and uniformity for the obtained front have a lower quality compared to the first case. This may be justified by the large side constraint of rotational speed used in this case. Same remarks of the first case have been deducted for the reference and optimized rotor that are shown in Figures 14(a) and 14(b), respectively.

*Configurations of the optimal machines obtained: T*able 8 shows the results of improvement made on efficiency and NPSHC at the nominal point. We observe:

- In the case of objective function form 1, performances were improved by 12.449 and 36.48%, respectively.
- In the case of form 2, the improvement of these two performances is 12.87 and 35.76%, respectively.
- In the case of form 3 and NSCS, the nominal efficiency was improved by 12.94 and 12.95%, respectively, while the nominal NPSHC was improved by 35.27% in both cases.

We also find in case 2 that all optimal tip radius tend to higher limit values, the diffusion factors resemble a free vortex, while we obtain an identical number of blades rotor for all optimized pumps.

*Evolution of machines' performances as a function of volumetric flow rate: I*n Figure 15, the performances of the machine according to the volumetric flow rate are presented. We observe a great convergence rate for the values of the performance with the optimized machines, exception is made to the solutions not belonging to the optimal Pareto front (objective function form 1). As in case 1, the optimized pumps have a high value of nominal efficiency with a large operating range (Figure 15(a)). We obtained that the hydraulic heads of the optimized pumps are higher than the reference values (Figure 15(b)). For the NPSH and

Table 7. Optimization results: case 1.

		CS			
Case 1	Reference pump	Form 1	Form 2	Form 3	NSCS
η_{nom} (%)	62.94	70.89	73.031	72.645	72.64
$NPSHC_{nom}$(m)	2.472	1.574	1.870	1.798	1.798
Q_v(m^3/h)	472.5	454.374	482.968	469.4472	469.886
R_i^1(m)	0.04	0.0302	0.0300	0.0300	0.0301
R_e^1(m)	0.125	0.15	0.1500	0.1500	0.1500
R_i^2(m)	0.04	0.0313	0.0300	0.0300	0.0301
R_e^2(m)	0.125	0.1492	0.1499	0.1498	0.15
D_i	0.3	0.6963	0.6952	0.6987	0.6833
D_e	0.5	0.4313	0.5395	0.5095	0.5073
Z	6	3	3	3	3

CS: cuckoo search; NPSHC: net positive suction head; NSCS: nondominated sorting cuckoo search.

Table 8. Optimization results: case 2.

		CS			
Case 2	Reference pump	Form 1	Form 2	Form 3	NSCS
η_{nom} (%)	62.94	70.7757	71.0431	71.086	71.093
$NPSHC_{nom}$(m)	2.472	1.570	1.5879	1.600	1.600
N (r/min)	840.00	891	883	884	884
R_e^1(m)	0.125	0.15	0.15	0.15	0.15
R_e^2(m)	0.125	0.1499	0.1489	0.1489	0.1489
D_i	0.3	0.6778	0.6182	0.5026	0.5050
D_e	0.5	0.3332	0.3573	0.5026	0.3584
Z	6	3	3	3	3

CS: cuckoo search; NPSHC: net positive suction head; NSCS: nondominated sorting cuckoo search.

NPSHC shown in Figure 15(c) and (d), respectively, we observe that, for the entire flow rate range, the optimized machines have smaller required suction capacities than the reference values with an obvious discrepancy, whereas for the NPSH, the difference between the curves is not evident over the entire range of the flow rate. Finally, at the nominal point, Figure 15(e) and (f) shows clearly that the energy absorbed by the three similar optimized machines is greater than the values of reference machine by around 15.4 and 19.77% by machine of form 1.

Conclusion

In this work, a multiobjective design optimization of the mono-rotor axial flow pump was presented using two approaches: the CS algorithms and the nondominated sorting CS, coupled with the inverse design. The targeted performances to be improved at the nominal point are the total efficiency and the required NPSHC. Two cases were studied, while taking into account the high number of constraints. The first case studied has eight variables: the initial theoretical flow rate, hub and tip radius at the inlet and outlet of the rotor, the diffusion factors at the hub and tip of the rotor, and the number of rotor blades. In the second case, the hub radius values at the inlet and outlet of the rotor and the initial theoretical flow rate have fixed values. The following variables will be kept as variables: rotation speed, tip radius, diffusion factors, and the number of rotor blades. In the bi-objective approach with the standard CS version, three forms of objective functions have been used. The results obtained allow us to draw the following conclusions:

1. All pump configurations optimized with the above mentioned approaches show a great improvement on the efficiency and the NPSHC compared to the reference pump. As for the other performances, at the nominal point, almost all the optimized pumps have values extremely close to each other. We draw the attention of the observer on the power absorbed; these pumps absorb more power compared to the reference. Finally, the performance of optimized machines has an extended range of operations compared to the reference machine.

2. The objective function according to form 3 which tends to draw the solution toward the ideal point shows its efficiency and can be used as a convergence test of the Pareto front. The standardization technique in forms 2 and 3 gives better results than those of form 1.
3. Compared to the standard CS and GA, in the case of the multiobjective optimization of turbomachines with a large number of constraints and relatively large side constraints, the NSCS with its diversity and uniformity indexes proves its rigor and precision.
4. The configuration chosen in case 1 is favorable for the optimization of the efficiency, while the one used in the second case is favorable for the optimization of the NPSHC.
5. Compared to the reference pump the total nominal efficiency and the NPSHC were improved by 15.42 and 27.26%, respectively (case 1, form 3 and NSCS, Table 7).

As part of the extension of this work, other objective functions can be added by formulating a problem of three or more objectives, for which other algorithms can be tested and compared with NSCS like NSGAIII, NSTLBO, and NSPSO.

Declaration of Conflicting Interests

The author(s) declared no potential conflicts of interest with respect to the research, authorship, and/or publication of this article.

Funding

The author(s) received no financial support for the research, authorship, and/or publication of this article.

ORCID iD

Mohamed Abdessamed Ait Chikh http://orcid.org/0000-0002-4032-4443

References

1. Srinivas N and Deb K. Multiobjective optimization using nondominated sorting in genetic algorithms. *Evolut Comput* 1994; 2: 221–248.
2. Coello CAC, et al. A comprehensive survey of evolutionary-based multiobjective optimization techniques. *Knowl Inf Syst* 1999; 1: 129–156.
3. Massardo A and Satta A. Axial flow compressor design optimization. part I: Pitchline analysis and multivariable objective function influence. *Journal of Turbomachinery* 1990; 112(3): 399–404.
4. Massardo A, Satta A and Marini M. Axial flow compressor design optimization: Part ii-throughflow analysis. *Journal of Turbomachinery* 1990; 112(3): 405–410.
5. Kipouros T, Jaeggi D, Dawes B, et al. Multi-objective optimisation of turbomachinery blades using tabu search. In: *International conference on evolutionary multi-criterion optimization*, pp.897–910. Berlin: Springer.
6. Benini E. Three-dimensional multi-objective design optimization of a transonic compressor rotor. *J Propul Power* 2004; 20: 559–565.
7. Samad A and Kim K. Shape optimization of an axial compressor blade by multi-objective genetic algorithm. *Proc IMechE, Part A: J Power and Energy* 2008; 222: 599–611.
8. Bonaiuti D and Zangeneh M. On the coupling of inverse design and optimization techniques for the multiobjective, multipoint design of turbomachinery blades. *J Turbomach* 2009; 131: 021014.
9. Kim JH, Choi JH, Husain A, et al. Performance enhancement of axial fan blade through multi-objective optimization techniques. *J Mech Sci Technol* 2010; 24: 2059–2066.
10. Takayama Y and Watanabe H. Multi-objective design optimization of a mixed-flow pump. In: *ASME 2009 fluids engineering division summer meeting*, pp.371–379. New York: American Society of Mechanical Engineers.
11. Wang X, Hirsch C, Kang S, et al. Multi-objective optimization of turbomachinery using improved NSGA-II and approximation model. *Comput Methods Appl Mech Eng* 2011; 200: 883–895.
12. Zhang J, Zhu H, Yang C, et al. Multi-objective shape optimization of helico-axial multiphase pump impeller based on NSGA-II and ANN. *Energy Convers Manag* 2011; 52: 538–546.
13. Chenxing ZLWSH and Qian Z. Multi-objective optimization design and experimental investigation of centrifugal fan performance. *Chin J Mech Eng* 2013; 26: 1.
14. Meng F, Dong Q, Wang P, et al. Multiobjective optimization for the impeller of centrifugal fan based on response surface methodology with grey relational analysis method. *Adv Mech Eng* 2014; 6: 614581.
15. Stadler M, Schmitz MB, Laufer W, et al. Inverse aeroacoustic design of axial fans using genetic optimization and the lattice-Boltzmann method. *J Turbomach* 2014; 136: 041011.
16. Yang W and Xiao R. Multiobjective optimization design of a pump–turbine impeller based on an inverse design using a combination optimization strategy. *J Fluids Eng* 2014; 136: 014501.
17. Huang R, Luo X, Ji B, et al. Multi-objective optimization of a mixed-flow pump impeller using modified NSGA-II algorithm. *Sci China Technol Sci* 2015; 58: 2122–2130.
18. Smith AE, Coit DW, Baeck T, et al. Penalty functions. *Evolut Comput* 2000; 2: 41–48.
19. Deb K. *Multi-objective optimization using evolutionary algorithms*. New York: John Wiley & Sons Inc., 2001.
20. Ait Chikh MA, Belaidi I, Khelladi S, et al. Efficiency of bio-and socio-inspired optimization algorithms for axial turbomachinery design. *Appl Soft Comput* 2018; 64: 282–306.
21. Robert R, Ricardo N and Bakir F. Pompes rotodynamiques – aérohydrodynamique des profils et aubages de pompes hélices. *Techniques de l'Ingénieur, Réf: BM4304 V1*, 2013.
22. Robert R, Ricardo N and Bakir F. Pompes rotodynamiques – dimensionnement et analyse des performances des pompes hélices. *Techniques de l'Ingénieur, Réf: BM4305*, 2013.

23. Nadir M, Ghenaiet A and Carcasci C. Thermo-economic optimization of heat recovery steam generator for a range of gas turbine exhaust temperatures. *Appl Therm Eng* 2016; 106: 811–826.
24. Grodzevich O and Romanko O. Normalization and other topics in multi-objective optimization. In: *Proceedings of the Fields MITACS industrial problems workshop*, pp.89–102. Toronto: The Fields Institute.
25. Deb K, Pratap A, Agarwal S, et al. A fast and elitist multiobjective genetic algorithm: NSGA-II. *IEEE Trans Evolut Comput* 2002; 6: 182–197.
26. Yang XS and Deb S. Engineering optimisation by cuckoo search. *Int J Math Model Numer Optim* 2010; 1: 330–343.
27. Yang XS and Deb S. Cuckoo search via Lévy flights. In: *World congress on nature & biologically inspired computing, 2009. NaBIC 2009*, pp.210–214. New York: IEEE.
28. Yang XS. *Nature-inspired metaheuristic algorithms*. Bristol: Luniver Press, 2010.
29. Yang XS and Deb S. Multiobjective cuckoo search for design optimization. *Comput Oper Res* 2013; 40: 1616–1624.
30. Wang Q, Liu S, Wang H et al. Multi-objective cuckoo search for the optimal design of water distribution systems. In *Civil engineering and urban planning 2012*. American Society of Civil Engineers, 2012. pp. 402–405.
31. Rani KA, Malek MFA, Neoh SC, et al. Hybrid multi-objective optimization using modified cuckoo search algorithm in linear array synthesis. In: *Antennas and propagation conference (LAPC)*, 2012 Loughborough, pp.1–4. New York: IEEE.
32. Fister I Jr, Yang XS, Fister D, et al. Cuckoo search: a brief literature review. In: Yang Xin-She (ed.) *Cuckoo search and firefly algorithm,* Berlin: Springer, 2014, pp.49–62.
33. He XS, Li N and Yang XS. Non-dominated sorting cuckoo search for multiobjective optimization. In: *2014 IEEE symposium on Swarm intelligence (SIS)*, pp.1–7. New York: IEEE.
34. Lei D and Wu Z. Pareto archive multi-objective particle swarm optimization. *Pattern Recognit Artif Intell* 2006; 19: 475–480.
35. Reyes-Sierra M and Coello CC. Multi-objective particle swarm optimizers: a survey of the state-of-the-art. *Int J Comput Intell Res* 2006; 2: 287–308.
36. Yao X, Liu Y and Lin G. Evolutionary programming made faster. *IEEE Trans Evolut Comput* 1999; 3: 82–102.
37. Laguna M and Martí R. Experimental testing of advanced scatter search designs for global optimization of multimodal functions. *J Global Optim* 2005; 33: 235–255.
38. Schaffer JD. Multiple objective optimization with vector evaluated genetic algorithms. In *Proceedings of the First International Conference on Genetic Algorithms and Their Applications, 1985*. (pp. 93–100). Lawrence Erlbaum Associates. Inc., Publishers.
39. Fonseca CM and Fleming PJ. An overview of evolutionary algorithms in multiobjective optimization. *Evolut Comput* 1995; 3: 1–16.
40. Deb K and Agrawal RB. Simulated binary crossover for continuous search space. *Complex Syst* 1994; 9: 1–15.
41. Cheikh M, Jarboui B, Loukil T, et al. A method for selecting pareto optimal solutions in multiobjective optimization. *J Informat Math Sci* 2010; 2: 51–62.
42. Deb K, Chaudhuri S and Miettinen K. *Estimating nadir objective vector quickly using evolutionary approaches*. Technical report, Technical Report KanGAL Report, Kanpur India, 2005.
43. Deb K, Miettinen K and Sharma D. A hybrid integrated multi-objective optimization procedure for estimating nadir point. In: *International conference on evolutionary multi-criterion optimization*, pp.569–583. Berlin: Springer.
44. Bechikh S, Said LB and Ghedira K. Estimating nadir point in multi-objective optimization using mobile reference points. In: *2010 IEEE Congress on Evolutionary Computation (CEC)*, pp.1–9. New York: IEEE.
45. Miettinen K. *Nonlinear multiobjective optimization*. vol 12, Berlin: Springer Science & Business Media, 2012.